Growth Dynamics of Fetal Human Neural Stem Cells

Walter D. Niles, Dustin R. Wakeman, and Evan Y. Snyder

Abbreviations

bFGF	Basic fibroblast growth factor (fibroblast growth factor 2)
DMSO	Dimethylsulfoxide
PBS	Dulbecco's phosphate-buffered saline
ECM	Extracellular matrix
EGF	Epidermal growth factor
FBS	Fetal bovine serum
hNSC	Human neural stem cells
LIF	Leukemia inhibitory factor

Introduction

Neural stem cells isolated from human fetal and adult sources have been propagated and expanded in culture to provide research platforms for understanding control of nervous system development and their potential as therapies for neural injury and diseases [1–5]. When transplanted into diseased hosts, human neural stem cells (hNSC) interact strongly with the pathological microenvironment, migrating to loci of nervous system injury, differentiating to replace damaged neurons and glia, restoring homeostasis to damaged cells, and delivering chemotherapeutic agents [6]. Culture methods that facilitate biological mechanisms favoring engagement of hNSC with cues in the host-diseased microenvironment to enact migratory and regenerative programs are critical for realizing this therapeutic potential. Fostering retention and control of the inherent developmental properties of NSC crucial to the therapeutic potential of NSC—multipotency, the ability to differentiate to the different cell types of the nervous system, and self-renewal, the ability to undergo mitosis to multipotent daughter cells—is thus of intense interest. From a practical standpoint, producing large populations of hNSC is needed for understanding not only the therapeutic potential of hNSC but also how the cellular milieu influences expression of these developmental programs.

hNSC are cultured ex vivo in neurospheres [5, 7–10], monolayers [5, 11, 12], and multilayers [13]. Isolated cells introduced to a culture vessel aggregate and proliferate as free-floating suspended masses that exhibit minimal interaction with nonadhesive substrates [5]. These "neurospheres" may grow both by proliferation of individual cells within each sphere and by "fusion" of nearby spheres into masses populated by thousands to millions of cells that interact strongly with each other by the secretion of cell adhesion and extracellular matrix (ECM) molecules. Neurosphere culture remains a popular and standard technique for NSC propagation, but is criticized as being neither a unique property of neural stemness [10, 14] nor an indicator of clonal proliferation [15]. From a technical standpoint, the physical nature of the neurosphere mass of cells has led to difficulties in controlling stem cell differentiation by external factors in the bathing medium due to the nonuniformity of exposure throughout the cell mass. Furthermore, propagation is inherently limited by the consumption of nutrients by outer cells at the expense of inner cells, such that spheres eventually form dead cores that diminish culture yield as necrosis competes with mitosis [11, 16].

Electronic supplementary material
The online version of this chapter (doi:10.1007/978-1-4614-7696-2_5) contains supplementary material, which is available to authorized users.

Disclosure: Walter D. Niles, Ph.D., is cofounder, co-owner, and chief scientific officer of Etaluma, Inc., which manufactures the incubator microscope used for time-lapse microphotography in this study.

W.D. Niles
Sanford Consortium for Regenerative Medicine, Sanford Burnham Medical Research Institute, 2880 Torrey Pines Scenic Drive, La Jolla, CA 92037, USA
e-mail: wniles@burnham.org

D.R. Wakeman
Department of Neurological Sciences, Rush Medical College, 1750 West Harrison Street, Cohn Building, Suite 347, Chicago, IL 60612, USA

E.Y. Snyder (✉)
Sanford Burnham Medical Research Institute, 10901 North Torrey Pines Road, La Jolla, CA 92037, USA
e-mail: esnyder@burnham.org

S. Sell (ed.), *Stem Cells Handbook*, DOI 10.1007/978-1-4614-7696-2_5,

Monolayer culture is induced by preventing neurosphere formation through seeding at a low density to decrease intercellular interactions [11, 12]. Plastic or glass substrates are often coated with biomolecules enabling NSC adhesion to the substratum, including poly-L- or D-lysine, poly-L- or D-ornithine, and ECM constituents such as fibronectin or laminins [12, 17]. Monolayer culture has also been obtained without adhesion-enabling biomolecules on corona discharge- or other ion plasma-treated surfaces, termed "tissue culture-treated," when cells are seeded at low density [1, 7]. Monolayer culture is favored because all the cells have ostensibly unimpeded access to growth factors and nutrients in the medium. It has revealed that basic fibroblast growth factor (bFGF, FGF2) and leukemia inhibitory factor (LIF) are the only growth factors required to maintain self-renewal and multipotency of hNSC isolated from fetal telencephalon [7, 18, 19] such that they differentiate into neuronal and glial subtypes appropriate to the target brain region when engrafted into the nervous system of living mammals [1]. This has allowed formulation of chemically defined culture media lacking serum [1, 2, 19].

This laboratory has developed methods for culture of fetal telencephalon-derived hNSC in multilayers by seeding on tissue culture-treated but otherwise unmodified plastic surfaces at relatively high densities [13]. Multilayers are intermediate between monolayers and neurospheres—cells interact with each other in local aggregations or clusters but also with the substrate via lamellipodia extending toward adjacent cell clusters. Proliferation expands the cluster area horizontally along the substrate as well as vertically in each expanding cluster. Migration of cells between clusters along the lamellipodia and subsequent proliferation is hypothesized to eventually unify previously discrete clusters. This culture mode produces large numbers of hNSC compared to both neurospheres and monolayers with the resulting cells suitable for differentiation control and transplantation. As culture of hNSC in multilayers is much less studied than monolayers and neurospheres, the present work explores quantitative parameters for successful propagation and maintenance of hNSC in this culture modality. Understanding these parameters will further acceptance of this technique for the realization of these advantages.

Materials and Methods

hNSC Source and Derivation

The hNSC used in this study, HFB 2050, were isolated from the telencephalon of a 13-week-old human fetal cadaver [1]. NSC were selected by serial culture in serum-free DMEM/F12 culture medium supplemented with N2 (Life Technologies, Carlsbad, CA), 5 mM L-glutamine, and 10 ng/mL LIF. Culture media alternated between 20 ng/mL bFGF (FGF2) and 20 ng/mL epidermal growth factor (EGF) to induce reentry into the cell cycle and to maintain the cells in a state of early neuroglial multipotentiality [17]. This procedure required six enzymatic passages before cryopreservation in 10 % (v:v) DMSO, 50 % FBS, 40 % culture medium. Cells were maintained thereafter in defined, serum-free conditions as described [13, 20, 21].

NSC Culture

Culture Conditions

Procedures previously described for multilayer culture of these cells were followed [21]. For this study, cryopreserved aliquots of cells from the original derivation were thawed and diluted sevenfold in culture medium of the following defined composition: Neurobasal medium (Life Technologies), Vitamin A-free B27 supplement (Life Technologies, Carlsbad, CA), 5 mM L-alanyl-L-glutamine (GlutaMax, Life Technologies), 20 ng/mL bFGF (R&D Systems, Minneapolis, MN), 10 ng/mL LIF (Millipore, Temecula, CA), 8 µg/mL heparin (Sigma-Aldrich, St. Louis, MO), and 2 µL/mL Normocin (Invivogen) [13, 21]. After collection of the cells by centrifugation at 200 rcf for 4 min, cells were resuspended in medium and cultured at 37 °C in humidified air containing 5 % CO_2 in 6- and 12-well plates, and T25, T75, and T225 flasks fabricated of tissue culture-treated polystyrene (Cat. No. 430639, 430641, and 3001, respectively, Corning Costar).

Dissociation and Collection of Cells for Passage

Cells were passed by aspiration of medium and one wash with Dulbecco's phosphate-buffered saline (PBS) followed by incubation in a volume of Accutase equal to one-fourth of the normal culture medium volume at 37 °C for 45 s. Lifting and dispersion of multilayers was then observed by light microscopy with gentle agitation of the culture vessel as described [13, 21]. Cells were dissociated to single cells and small aggregates (≤5 cells) by triturating 2 or 3 times with a 5 mL disposable pipette, taking care to avoid undue shear stress, and transferred to a 15 mL conical polypropylene centrifuge tube. Total time in Accutase was confined to <2 min. Enzyme was quenched by dilution with 6 volumes of culture medium used to wash the culture vessel, and cells were pelleted by centrifugation at 200 rcf for 4 min at room temperature. The pellet was resuspended in 1.0 mL culture medium by 2 triturations with an Eppendorf 1.0 mL pipetter.

Quantitation of Viable Cells

At each passage, viable cell densities were quantified by counting on a Neubauer hemocytometer. Typically 2 µL of cell pellet resuspension was diluted 1:50 with PBS, and then an equal volume of 0.4 % Trypan Blue was added for a final counting dilution of 1:100. Cells exhibiting a bright white

boundary under phase contrast observation were scored as viable and used for seeding density and yield calculations.

Seeding New Culture Vessels and Feeding

New culture vessels were seeded with dispersed cells at a desired surface area density. Freshly seeded cultures were allowed to grow at 37 °C without mechanical disturbance (including movement for observation) for at least 3 and up to 5 days. The first feeding was a replacement of half the medium volume covering the cells with fresh medium containing twice the normal concentrations of supplementary growth factors, i.e., 40 ng/mL bFGF, 20 ng/mL LIF, and 16 μg/mL heparin. All medium replacements were performed by slow rotation of the vessel about its horizontal axis (e.g., taking 5–10 s) to move the liquid off the growth surface to avoid detachment of the cells by the meniscus and into a flask corner. After removal and replacement of the desired liquid volume, the vessel was subsequently slowly rotated back to allow the refreshed medium to cover the cells while avoiding meniscus shear. After this first feeding, cells were washed and the medium replaced every 3–5 days utilizing the same liquid removal and replacement maneuvers to avoid detaching the cells from the growth surface.

Coating Tissue Culture Vessels with Laminins

Culture vessels, including 6-well plates, T25, T75, and T225 flasks, were first coated by incubation in 10 μg/mL poly-l-ornithine (Sigma-Aldrich) in sterile PBS for 24 h at 37 °C. Unattached poly-L-ornithine was removed by three washes with sterile PBS at room temperature. The surfaces were subsequently coated with 10 μg/mL mouse laminins (Life Technologies) in PBS by incubation for 24 h at 37 °C. The incubation solution was removed, the surface washed once with PBS, and the flasks stored for use at 4 °C as described [11].

Time-Lapse Microphotography

Cells were plated on 35 mm diameter tissue culture-treated polystyrene Petri dishes for observation with a ×20/0.4 NA 4.5 mm working distance objective (Meiji Techno, Saitama, Japan), and plated on glass bottom 35 mm FluoroDishes (Cat. No. FD35, World Precision Instruments, Sarasota, FL) for observation with a ×40/0.65 NA 0.5 mm working distance objective. The seeding density was 10^5 cm^2 when the surface was untreated, and 4×10^4 cm^2 when the surface was coated with laminin. Cells were observed with a custom inverted fluorescence microscope having an integrated CMOS imager interfaced via USB 2.0 with a computer for display (Lumascope, EtaLuma, Inc., Carlsbad, CA). Cells were transilluminated in brightfield at an oblique angle through the plastic dish cover with a white LED on a flexible cable. After plating, the dish was placed on the stage of the microscope inside a 37 °C incubator, a field of view was brought into focus, and successive images were acquired and stored as bitmaps at time intervals of 5 or 10 min for a collection period of up to 14 days with custom software (LumaView). Image files were assembled into movies with Adobe Premier 6.5. In brief, each 4 MB bitmap image (1,280 × 800 pixels) in a time-lapse series was replicated into five successive video frames (760 × 480 pixels). The resulting sequence of video frames was compressed by an MPEG-1 codec into a movie for playback at 30 frames per second. Total time-lapse collection periods and movie durations are noted in each movie legend.

Results

NSC Growth in Multilayers and Monolayers: Intercellular Interaction with Continual Expression of Lamellipodia

Growth on Tissue Culture-Grade Polystyrene

When introduced to a fresh surface, dissociated hNSC grew into multilayers with a stereotypical pattern and time course. The seed of freshly dissociated cells shown in Fig. 1a, in which the plane of focus is located at the flask floor, consisted of single cells and small aggregates of ≤5 cells. After 3 days of undisturbed incubation at 37 °C, most cells had settled on the growth surface, aggregated into small colonies, and begun proliferating within these clusters (Fig. 1b, left). Some cells along the edges of each cluster extended lamellipodia along the growth surface. Lamellipodia extended from nearby colonies appeared to be directed toward each other, suggesting a chemosensory tropism. This surface exploratory behavior by elaboration of lamellipodia was critical for establishment of proliferating multilayer cultures. Cells remaining as singlets unassociated with any colony extended few, if any lamellipodia, suggesting minimal interaction with the surface. Settled cell clumps not expressing lamellipodia either did not proliferate or formed neurospheres that lifted away from the growth surface (Fig. 1b, right).

Between 3 and 5 days of incubation (Fig. 1c, left), colonies increased in mass by proliferation, resulting in the multilayer appearance. In addition, cells migrated, as if in "chains," along the exploratory lamellipodia established by cells near the peripheries of the colonies, especially lamellipodia that had come into contact with lamellipodia extended from adjacent colonies. Proliferation of these migratory cells resulted in establishment of "branches" or "chains." Continual migration and proliferation of cells both along and

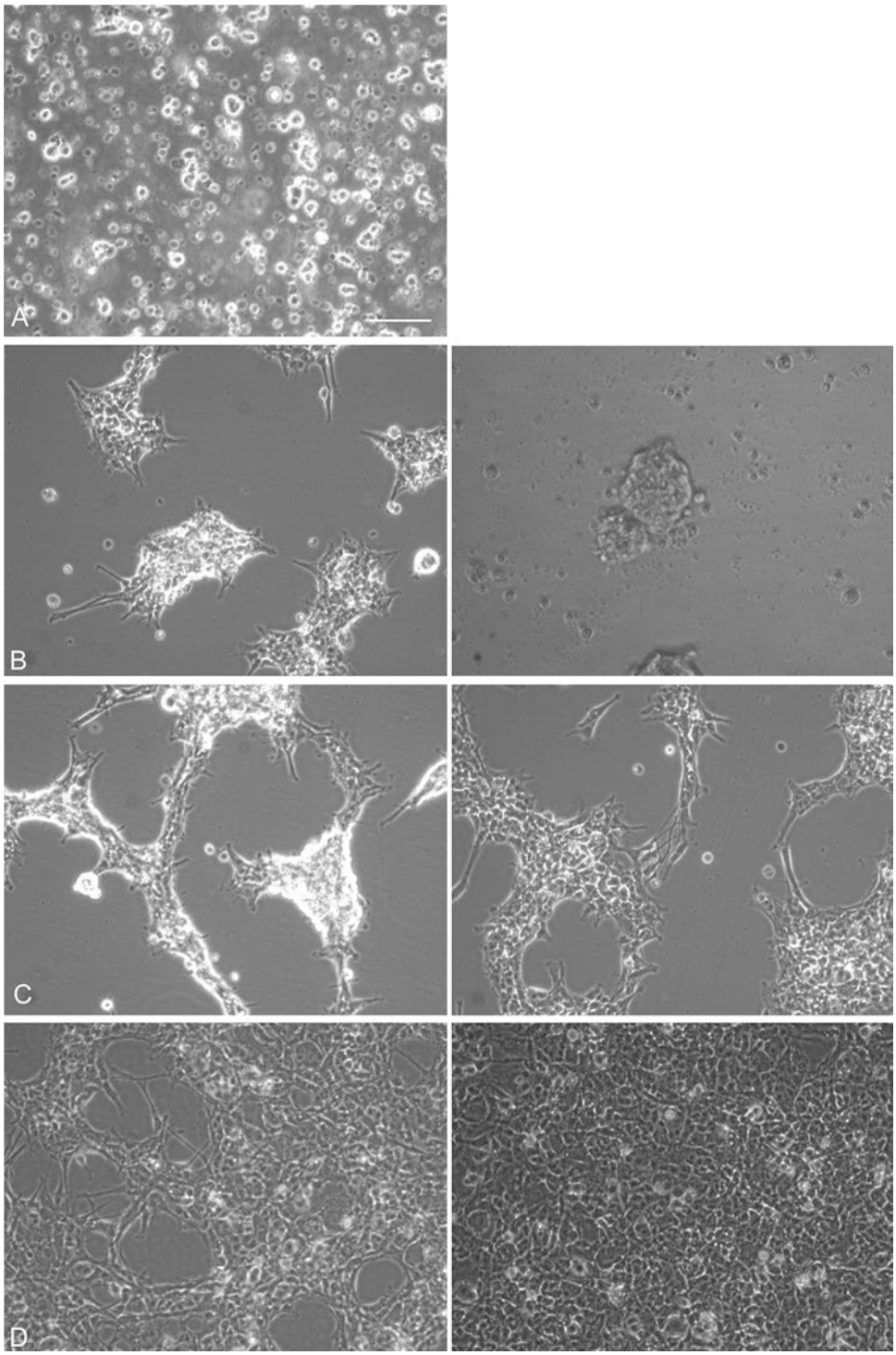

Fig. 1 Time course of fetal-derived hNSC multilayer growth on an uncoated, tissue culture-grade polystyrene surface. (**a**) Accutase-dispersed cells freshly seeded in a T25 flask in 6 mL medium at a surface area density of 1.3×10^5 cells/cm^2 (3.25 million cells total cells). While not all cells had settled to the flask floor, as seen by out-of-focus cell boundaries, their center-to-center spacing was consistent with an average separation of 15.6 ± 3.9 μm expected for the area density of the seed. (**b**) *Left*: after 3 days of mechanically undisturbed growth, cells have aggregated and begun to proliferate within each group. Cells have also begun to explore the growth surface by expression of lamellipodia. Lamellipodia from nearby groups appear to project toward each other. *Right*: cells 3 days after seeding at $<0.8 \times 10^5$ cells/cm^2 in a different T25 flask. These cells formed small clusters, did not extend lamellipodia, and died within 5 days of seeding, indicating that surface exploration was critical for survival. (**c**) *Left*: between 3 and 5 days of culture, cells migrate along exploratory lamellipodia and proliferate to form branches that connect adjacent colonies. *Right*: over days 5–7, cells continue to proliferate within colonies, and migrate and proliferate along branches established between colonies. (**d**) *Left*: By 7–10 days after seeding, expanding colonies merge into multilayers. *Right*: cells have grown to confluence by 2 weeks of growth. The plane of focus was positioned at the growth surface such that the boundaries of lamellipodia were the sharpest. Cells growing on top of surface-attached cells thus exhibit less sharp boundaries. Scale bar, 50 μm

within these branches and subsequent extension of new lamellipodia enabled further branch/chain migration and proliferation to increase coverage of the growth surface area.

Over days 5–7 (Fig. 1c, right), growth progressed by the colonies appearing to flatten, suggesting that daughter and sibling cells sought and established contact with the growth surface with the resultant crowding stimulating further area expansion. By 7–10 days of growth (Fig. 1d), many branches between colonies had merged creating a more uniform coverage of the growth surface by the cells to ~80 % confluence. Cells along colony peripheries continued to extend lamellipodia into unoccupied growth surface with concomitant chain and branch migration and proliferation. Growth continued in this highly stereotypical pattern until attaining confluence by 2 weeks (Fig. 1e).

This pattern of growth was observed independently of passage number for up to 43 passages, the greatest passage studied.

Time-Lapse Observation of hNSC Growth on Uncoated Surfaces

Movies of freshly seeded hNSC on glass surfaces revealed surprising dynamics underlying the stereotypical growth pattern time course sampled in static images. Over the first 24 h (Movies 1 and 2), cells were mobile in the fluid medium, suggesting Brownian motion [22] as is observed during the initial stage of neurosphere formation [5]. Cells jostled into one another to aggregate into colonies that eventually became stationary on the surface. During the subsequent 1–2 days, cells in these colonies became unipolar in shape, producing extensive lamellipodia along the surface in multiple directions from each colony. One of the most striking observations was that many lamellipodia extended by cells located along peripheries of colonies were temporary. These lamellipodia were extended relatively long distances and subsequently retracted to the cell soma over a period of ~30 min, suggesting chemotactile "sampling" of the surface. By the end of the third day, many lamellipodia became longer-lived—particularly those extending toward lamellipodia extending from an adjacent colony of cells. Lamellipodia from one colony that touched a smaller neighboring colony triggered a rearrangement of cells in the smaller colony along the apparently contacting lamellipodia, an event reminiscent of neurosphere fusion [5]. Individual cells often migrated away from colonies, and then migrated back to the original colony merging in a different location, or merging with a different colony. One notable point of contact was extended lamellipodia, such that as multiple cells migrated and grouped, a branch was created.

Growth on Laminin-Coated Polystyrene

When freshly dissociated hNSC were introduced to laminin-coated polystyrene, single cells and aggregates of cells grew as a discontinuous monolayer (Fig. 2). By 1 day after seeding, cells within clusters had begun flattening on the growth surface, adopting uni-, bi-, and multipolar shapes, and migrating with extensive lamellipodia (Fig. 2a). Over days 1–3, the flattening of cells increased their surface area occupancy, and cells migrated so as to disperse any initial clusters that had been previously formed (Fig. 2b). Cells continued to extend long lamellipodia and migrate resulting in prominent visible cytosol surrounding the nucleus of each cell with prominent lamellipodia (Fig. 2c). In contrast to growth as multilayers, cells on laminin underwent much less migration along lamellipodia established by other cells or clusters of cells grouping along pioneer lamellipodia. As a result, hNSC on laminin grew more as individual cells in small proliferation colonies, and clear unoccupied growth surface remained visible between adjacent cells for at least 12 days after seeding (Fig. 2d).

In time-lapse observation, cells remained as individuals immediately on seeding, settling on the growth surface and extending lamellipodia (Movies 3 and 4). Cells began rapid migration along the surface, continually making apparent contact with each other, but typically passing either over or under one another apparently to regain contact with the laminin-coated surface. As cells proliferated, nearby cells tended to remain close to one another resulting in small colonies of flattened adjacent cells. These colonies never resulted in the large extensive groupings of proliferated cells characteristic of growth in the multilayer pattern. Thus, cells seeded on laminin-coated surfaces began immediately to migrate along the surface, without undergoing extensive intercellular interactions as on uncoated surfaces.

Immunochemical Markers of Neuroglial Stemness

hNSC growing as multilayers on bare polystyrene and as monolayers on laminin stably expressed immunochemical markers of neural stemness and multipotency. All cells in cultures at 2 weeks stained positive for human nestin, the classical neural stemness marker whether cultured on uncoated (Fig. 3a) or laminin-coated polystyrene (Fig. 3c). Less than 5 % of cells stained for the neuronal marker doublecortin or the oligodendroglial marker O4 (not shown), indicating that these culture conditions did not favor differentiation to late, specific neuroglial lineages [13].

Cells throughout multilayer colonies expressed βIII-tubulin as indicated by positive staining with the monoclonal primary antibody clone TuJ1 (Fig. 3c). Staining was confined to long lamellipodia projecting from these peripheral cells. On laminin-coated surfaces, most cells stained positive for βIII-tubulin (Fig. 3d). While βIII-tubulin is generally regarded as a marker of neuronal commitment, it was

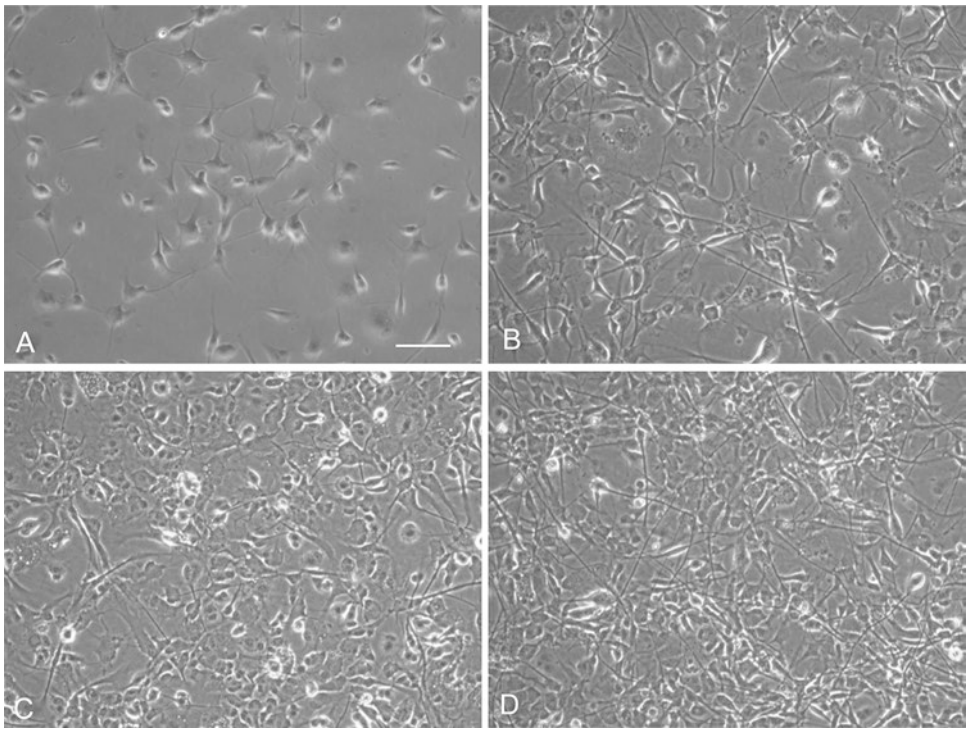

Fig. 2 Time course of fetal-derived hNSC growth on a laminin-coated tissue culture-grade polystyrene surface. (**a**) Cells 24 h (1 day) after seeding. Aggregates and colonies of cells expressed extensive lamellipodia exploring the growth surface. (**b**) Cells 3 days after seeding. Cells have migrated from clusters and attached to the laminin-coated surface to flatten. Each cell occupies greater surface area than comparative growth on uncoated polystyrene and expresses a greater profusion of lamellipodia. (**c**) Cells at day 7. The cells have established a discontinuous monolayer with unoccupied surface area between cells. (**d**) Cells at day 12 appear similar to cells at earlier times. Scale bar, 50 **μ**m

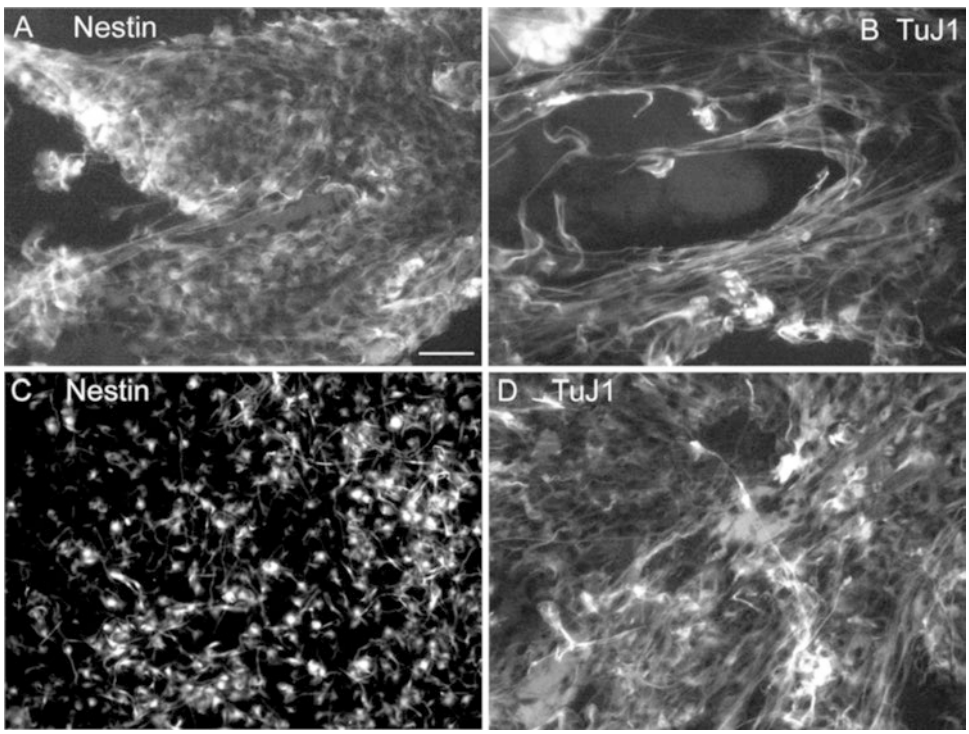

Fig. 3 Immunostaining of nestin (**a**, **c**) and **β**III-tubulin (TuJ1, **b**, **d**) of fetal hNSC grown as multilayers on uncoated tissue culture-grade polystyrene (**a**, **b**) and as monolayers on laminin-coated surfaces (**c**, **d**). Scale bar, 50 **μ**m

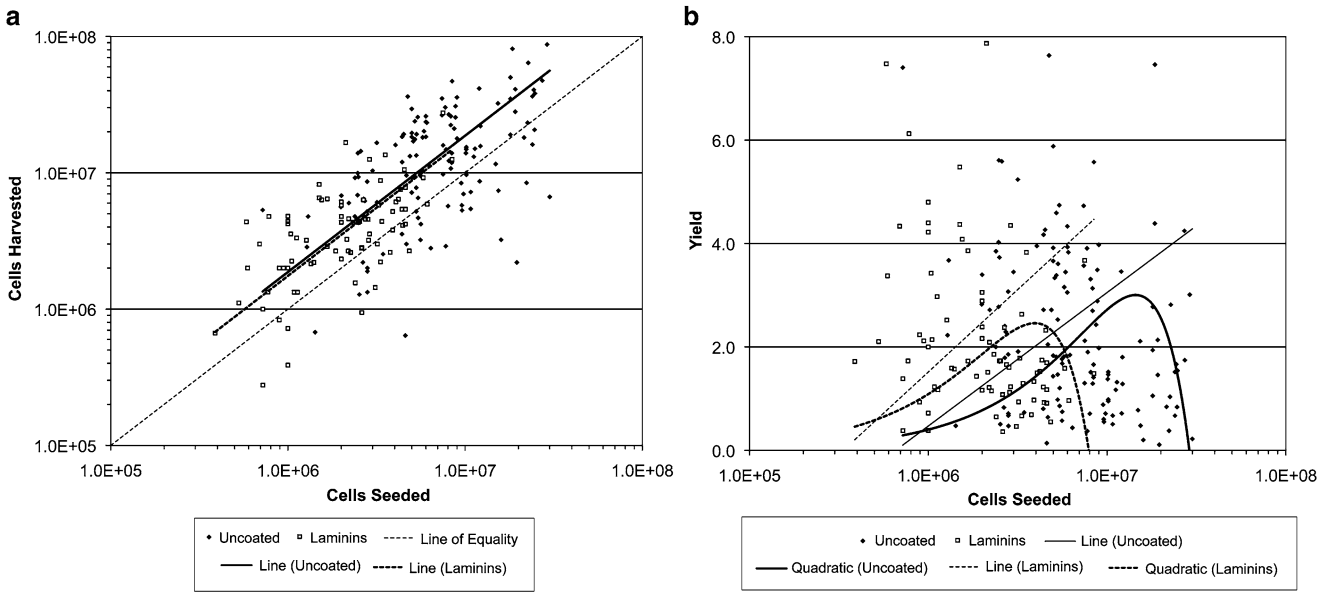

Fig. 4 Yields of hNSC cultured on uncoated and laminin-coated surfaces. (**a**) The number of viable cells harvested plotted as a function of the number of cells seeded into 242 uncoated (*filled diamond*) and 137 laminin-coated (*square*) culture flasks. Seed and harvest numbers ranged from 3×10^5 to 8.7×10^7. The abscissa and ordinate are represented with common logarithmic scales to give equal spatial representation on the graph across these orders of magnitude. The *dashed diagonal line* denotes the line of equality, in which the same number of cells were harvested as seeded. Lines through the data points (*solid line*, uncoated; finely *dashed line*, laminin-coated vessels) were obtained by linear regression of cells harvested on cells seeded, constrained by 0 cells harvested for 0 cells seeded. The slopes of these lines were not significantly different. (**b**) Yield, the number of cells harvested/the number of cells seeded, plotted as a function of the number of cells seeded for uncoated (*filled diamond*) and laminin-coated (*square*) vessels. The abscissa has logarithmic scale to provide equal graphical representation across of the range of seed size. The *upward sweeping lines* (*solid line*, uncoated; finely *dashed line*, laminin-coated vessels) were obtained by linear regression of yield on seed size, whereas the biphasic lines were least-squares minimization fits of a parabola to the data. Both fits were subject to the constraint of a yield of 0 for a seed size of 0. Parabolae provided significantly better description of yield as a function of seed size, indicating the requirement for an optimal number of cells to maximize yield

observed in nestin-positive NSC not expressing other markers of neuronal commitment. Therefore, βIII-tubulin may indicate an exploratory phenotype rather than specific lineage specification [23, 24].

Quantitative Parameters of hNSC Growth in Multilayers and Monolayers

Cell Yield

Seeding a vessel with a greater number of cells increased the number of cells harvested at passage. Each culture vessel was seeded with a counted number of viable cells, and viable cells were counted at passage. The number of cells at harvest is plotted in Fig. 4a as a function of the number of cells in the seed for 242 otherwise uncoated tissue culture-grade polystyrene vessels (*filled diamond*) and 79 vessels of the same type coated with laminin (*square*). Both axes of the plot are logarithmic to provide equal representation of the data across each power-of-ten of cell number. In general, fewer cells were seeded on laminin-coated surfaces compared to uncoated surfaces, due to the larger cell area on laminin at confluence. As denoted by points located above the dashed line of equality, representing the same number of cells harvested as seeded, more cells were harvested than seeded from 67.4 % of uncoated vessels and 82.3 % of laminin-coated vessels ($P<10^{-3}$, one-way ANOVA; $F=54.57$, uncoated; 19.45, laminin-coated). Linear regression of cells out on cells in (constrained by 0 cells out on the *y*-intercept for 0 cells in) yielded slopes of 1.8713 ± 0.1305 (uncoated, $R^2=0.2956$) and 1.7522 ± 0.4655 (laminin, $R^2=0.3287$). Within the modest goodness of fit, the slopes are not significantly different, indicating that these fetal hNSC grow similarly on both surfaces. More noteworthy were the strong correlation coefficients of 0.5554 (uncoated) and 0.5893 (laminin) between cells harvested and cells seeded. This indicates that >30 % of the variance in the number of cells harvested for the number cells seeded was accounted by the correlation between cells harvested and cells seeded, making the seed size the most significant predictor of cells obtained at harvest.

Yield, the number of cells at harvest per each cell seeded, was used to examine the roles of seed size and growth time in promoting cell growth. Cell yield was calculated as the

number of viable cells harvested from each vessel at passage divided by the original number of viable cells seeded in the vessel, i.e., yield = cells out at harvest/cells in at seed. Yields were plotted in Fig. 4b as a function of the number of cells seeded in uncoated (*filled diamond*) and laminin-coated (*square*) vessels. Average yield on laminin, 2.156 ± 1.546, was not significantly different than that on uncoated polystyrene, 2.308 ± 1.614 (*t* test, $P > 0.40$). The correlation coefficients between yield and seed size were –0.2252 for uncoated and –0.2826 for laminin-coated plastic, suggesting that seeding larger numbers of cells attenuated relative growth. Comparing fits of linear and parabolic functions to the data revealed that the biphasic parabola provided better goodness of fit between yield and seed size. Coefficients of determination R^2 increased from 0.0255 for the line to 0.4764 for the parabola for cultures in uncoated vessels and increased from 0.0654 for the line to 0.5421 for the parabola for cultures in laminin-coated vessels. Thus, yield was decreased both when too few or too many cells were seeded on either bare plastic or laminin-coated surfaces. While a linear relation between seed size and yield with slope >0 would suggest interactions between cells promoting proliferation, the better fits by parabolae indicate that an optimal number of seeded cells was necessary to maximize these interactions.

Period of Time in Culture and Doubling Times: No Effect of Laminin

The period of time elapsing between seed and harvest (growth time) resulting in greatest yield ranged between 7 and 21 days on bare polystyrene and between 5 and 14 days on laminins. Yield as a function of growth time is shown in Fig. 5a for uncoated (*filled diamond*) and laminin-coated polystyrene (*square*) for all vessels. Cells grown on laminin spread out such that each cell occupied greater surface area compared to growth as multilayers on uncoated polystyrene. Thus, cultures on laminin attain confluence earlier and were harvested after shorter growth periods. Yield initially increased the longer a culture was allowed to grow. For longer growth periods, yield decreased, consistent with contact inhibition of proliferation. Correlations between yield and growth time of 0.4463 for uncoated and 0.2037 for laminin-coated polystyrene made growth time the second most significant growth parameter after seed size.

To quantify growth dynamics of hNSC, the exponential growth function,

$$\frac{N_{\text{out}}}{N_{\text{in}}} = 2^{T/t_2} \qquad (1)$$

where T is the growth period, and N_{out} and N_{in} are cells harvested and cells seeded, respectively, was used to calculate the doubling time constant t_2 for vessels with yields >1. In this approach, the cells in each culture vessel are assumed to be a uniform population in which t_2 is the average time period elapsing between the birth of a cell by mitosis and its subsequent mitosis into two daughter cells and t_2 is stationary, that is, identical for each cell and constant during growth of the population. Yield, $N_{\text{out}}/N_{\text{in}}$, is thus predicted to be logarithmic with respect to growth time. Fitting exponential growth curves to the data of Fig. 5a decreased goodness of fit for cultures grown on uncoated surfaces ($R^2 = 0.1991$ for the line, 0.1838 for the exponential), and only slightly improved goodness of fit for cultures grown on laminin-coated surfaces ($R^2 = 0.0415$ for the line, 0.0503 for the exponential). More noteworthy, however, was that the slopes of linear relations between yield and growth time were not significantly different for the two growth surfaces (0.1151 ± 0.0203, uncoated; 0.0996 ± 0.0546, laminin-coated; $t = 0.2646$, $P > 0.40$). This suggests that cells on uncoated and laminin-coated surfaces proliferated at the same rate.

To test this hypothesis, it was necessary to determine that the assumptions underlying the simple doubling function model were applicable to hNSC growth on both surfaces. Doubling times t_2 calculated for each culture vessel were shown as frequency histograms for both growth surfaces in Fig. 5b. Dividing the growth time T of each harvested culture by the doubling time t_2 calculated for that culture results in a normalized growth time T/t_2. Plotting each culture's yield against its normalized growth time revealed that all points obtained on both growth surfaces were coincident along the same line having a slope indistinguishable from log(2.0) (Fig. 5c) with excellent goodness of fit ($R^2 = 0.9992$), indicating validity of the assumptions underlying the doubling model for growth on both uncoated and laminin-coated surfaces.

Distributions of t_2 for uncoated and laminin-coated polystyrene substrates shown in Fig. 5d revealed no effect of laminin on growth rate. Doubling time t_2 was not significantly greater for cultures grown on uncoated polystyrene (average ± SD, 13.660 ± 11.461 days) compared to laminin (13.193 ± 13.339 days) by both parametric (*t* test, $P > 0.8$) and nonparametric (Kolmogorov–Smirnov test, $P > 0.60$) tests. Furthermore, restricting the comparison to the 80 % fastest growing cultures in each group, to exclude cultures that might have experienced unknown anomalous conditions contributing to abnormally slow growth, did not result in a significant difference in t_2 (9.260 ± 3.387 days, uncoated; 6.939 ± 3.527 days, laminin; *t* test, $P > 0.30$). Thus, laminin does not act as a growth factor for hNSC.

Inverse Correlation Between Doubling Time and Yield

Yield and doubling time t_2 measured for individual cultures were strongly correlated on both types of growth surfaces. As shown in the plot of yield as a function of doubling time in Fig. 6, greater yields were obtained with shorter t_2.

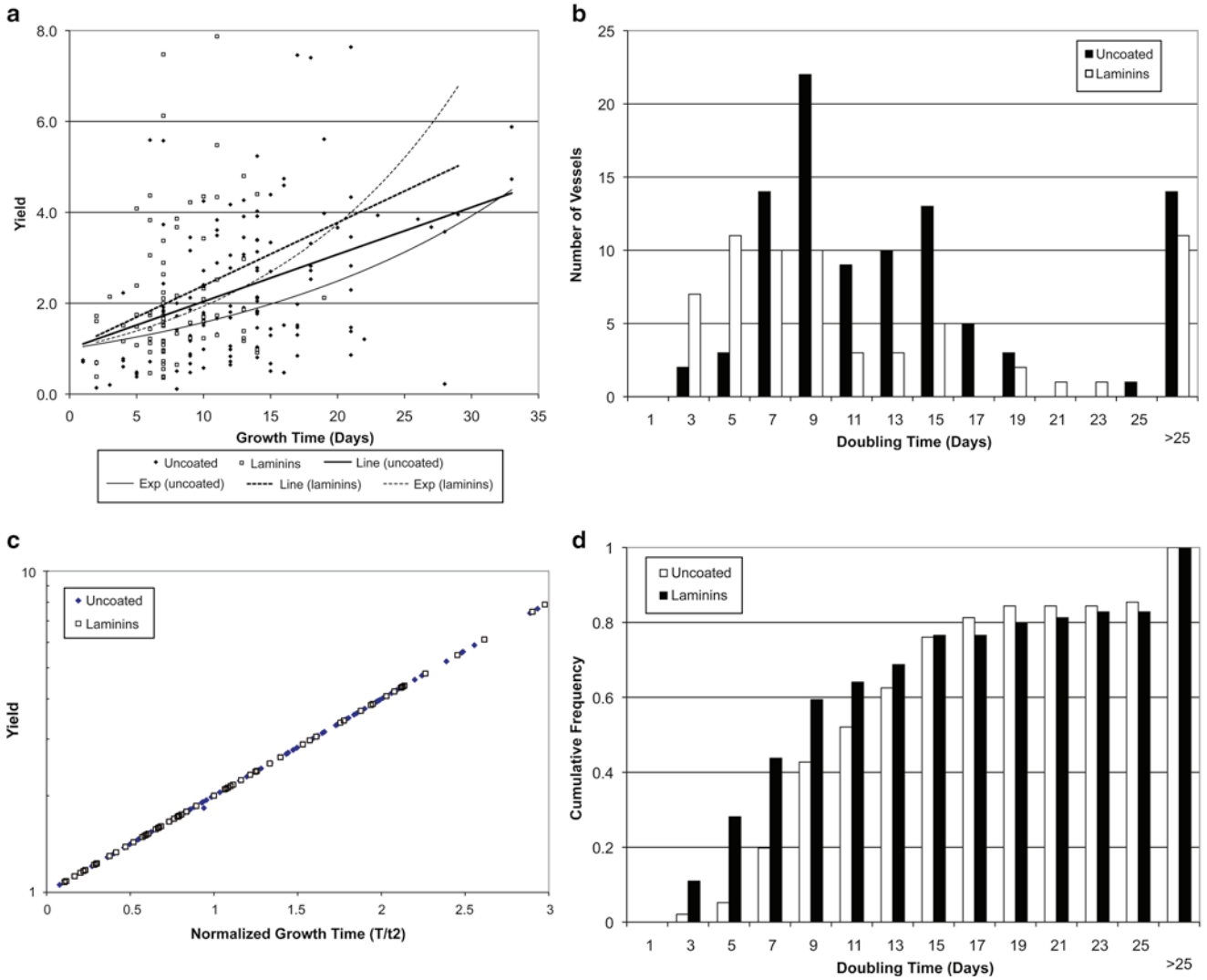

Fig. 5 Growth rates of hNSC on uncoated and laminin-coated surfaces. (**a**) Yield plotted as a function of time elapsing between seed and harvest (growth time) for hNSC seeded on uncoated (*filled diamond*) and laminin-coated (*square*) surfaces. *Straight lines* (*solid*, uncoated, yield = $0.1037T + 1$; *dashed*, laminin-coated, yield = $0.1386T + 1$) were obtained by linear regression of yield on growth time subject to the constraint of yield = 1.0 for a growth time of 0 days. The upwardly *curved lines* (*solid*, uncoated, yield = $2^{0.0656T}$; *dashed*, laminin-coated, yield = $2^{0.0952T}$) were obtained by least-squares fitting of the exponential doubling function, yield = $2^{\text{constant T}}$ to the data. (**b**) Frequency histograms of the doubling time t_2 calculated from (1) for hNSC grown on uncoated (*open columns*) and laminin-coated (*closed columns*) polystyrene vessels. (**c**) Validity of exponential growth model for proliferation of hNSC on uncoated (*filled diamond*) and laminin-coated (*square*) surfaces. For each culture, growth time T was divided by t_2 calculated from (1), and the culture yield was plotted as a function of this normalized growth time. The best-fitting line ($R^2 = 0.9992$) has slope $\log_{10}(2) = 0.30103$, indicating consistency of hNSC growth on both uncoated and laminin-coated polystyrene surfaces with the exponential growth model of (1). (**d**) Frequency distributions of doubling time t_2 on uncoated (*square*) and laminin-coated (*filled square*) surfaces

The correlation coefficients were –0.342 on polystyrene and –0.566 on laminins. The increased correlation on laminin is consistent with the relatively rapid surface spread of the cells into a monolayer within the 3-day period during which cells on uncoated polystyrene gradually underwent aggregation into colonies and attached to and explored the surface. This faster spread attenuated yields on laminin with respect to those obtained with uncoated polystyrene as cells proliferated horizontally on the laminin-coated surface and attained confluence with a decreased number of cells rather than both horizontally and vertically within and at the peripheries of the multilayer colonies formed on uncoated surfaces.

Growth dynamics of hNSC on uncoated and laminin-coated polystyrene were not significantly different by analysis of yield dependence on t_2. Least-squares analysis was used to fit exponential and polynomial functions to the data of Fig. 6. Single exponential functions (see Fig. 6) provided the best fits, $R^2 = 0.3962$ for polystyrene and 0.4630 for laminins.

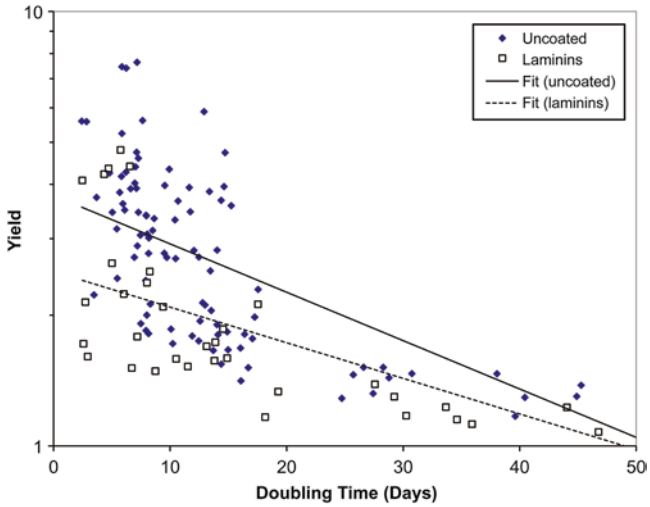

Fig. 6 Yield as a function of doubling time t_2 for hNSC growth on uncoated (*filled diamond*) and laminin-coated (*square*) surfaces. The curves (*solid*, uncoated; *dashes*, laminin-coated) are best-fitting exponential functions of the form $\text{yield} = a \times 2^{-b\,t_2}$. Best fitted parameters: uncoated polystyrene, $a = 3.7701 \pm 0.4414$, having units of yield which is dimensionless, and $b = 0.0369 \pm 0.0123$ days ($R^2 = 0.3962$); laminin-coated surfaces, $a = 2.5195 \pm 0.5215$ and $b = 0.0273 \pm 0.0242$ days ($R^2 = 0.4630$). The b or slope parameter did not significantly differ between the two surfaces (two-sided $P > 0.36$, $t = 0.3558$, 112.374 degree of freedom by the Welch–Satterthwaite equation). The yield intercepts a, where the fitted lines intersect the yield ordinate at 0 doubling time, tested significantly different (one-sided $P < 0.04$, $t = 1.8304$, dof = 156.27). This is consistent with decreased yield on laminin without change in the hNSC growth rate

More complicated functions did not improve goodness of fit. For example, double exponential functions resulted in $R^2 = 0.3749$ for polystyrene and 0.4372 for laminins. The best fits of polynomial functions of the form $\text{yield} = \sum_{i=1}^{n} a_i (t_2)^n$ were obtained with the highest order tested, $n = 6$, resulting in $R^2 = 0.366$ for polystyrene and 0.447 for laminins. Rate constants of the single exponential functions for uncoated (average ± SEM, 0.0369 ± 0.0123 days) and laminin-coated polystyrene (0.0273 ± 0.0242) were not significantly different (two-sample t test with unequal variances and sample sizes, $P > 0.36$). Thus, laminin did not change the proliferation rate of fetal-derived hNSC as measured by the dependence of yield on doubling time.

Surface Seeding Density Dependence of Yield and Doubling Time

Yield was strongly dependent on the number of cells seeded per unit surface area of growth surface (the seeding density) for both uncoated and laminin-coated vessels, having correlation coefficients of −0.2561 and −0.2042. The greatest yields of hNSC grown in multilayers on uncoated polystyrene surfaces were obtained by seeding within a range between 0.8 and 1.2×10^5 cm^2. For cultures seeded in this range, yields were >2.0 in >50 % of cultures for all growth periods (Fig. 7a). Seeding outside of this range resulted in decreased yields. At lower seeding densities, e.g., $< 0.6 \times 10^5$ cm^2, cells aggregated into small colonies that did not express exploratory lamellipodia (Fig. 1b, right). These colonies proliferated at rates too slow to overcome cell death, which decreased yield to <1.0. Seeding densities $> 1.2 \times 10^5$ cm^2 resulted in aggregation of cells into large neurosphere-like colonies within several days. While these colonies typically flattened on the growth surface and engaged in the multilayer pattern of proliferation, they sometimes detached from the substrate to form neurospheres. The attached colonies were large enough to attenuate access of interior cells to nutrients in the extracellular medium and decrease yield. Even greater seeding densities (e.g., $> 1.6 \times 10^5$ cm^2) favored more rapid aggregation into larger neurospheres, which would detach from the surface, never form multilayers, resulting in decreased yield, consistent with the negative correlation between yield and seeding density.

Growth on laminin-coated polystyrene shifted the optimum seeding surface density to a lower range such that fewer cells were necessary to evoke proliferation. Seeding densities as low as 5×10^3 cm^2 resulted in yields >1.0, and decreases in yield were not obtained until cells were plated at densities $> 1.2 \times 10^5$ cm^2 (Fig. 7a).

These biphasic functional relationships between seeding density and yield for both uncoated and laminin-coated surfaces revealed complexities in the interactions between cells determining yield. As these intercellular interactions are encapsulated formally in the seeding density, polynomials of the form $\text{yield} = \sum_{i=1}^{n} a_i (\text{density})^i$ were fitted to the data, where the a_i are coefficients indicating the strength of each order term in density, and omission of the zeroth order term ($n = 0$) constrained each fit to 0 yield for a seeding density of 0. Linear fits ($n = 1$) were interpreted as a simple paracrine interaction in which each cell secretes diffusible or surface-attached growth factors promoting proliferation of itself and neighboring cells by a non-saturable interaction. Lines exhibited the worst goodness of fit for both surfaces, however ($R^2 = 0.002$, uncoated; 0.0009, laminin-coated; see Table 1), indicating that the intercellular interactions underlying the surface density effect were more complicated than could be described by a simple linear model. Goodness of fit was improved most greatly by increasing the order of fitted polynomial to $n = 2$, which describes the biphasic relationship as a parabola. R^2 was 0.0400 for uncoated surfaces and 0.0286 for laminin-coated surfaces, denoting improvement of the parabola in describing yield as a function of seeding density compared to a line by factors of 20 and 32, respectively. Increasing the order of the fitted polynomials improved goodness of fit by a proportionally decreasing amount by providing local maxima most closely coinciding with the observed optimum seeding densities. While polynomials up to

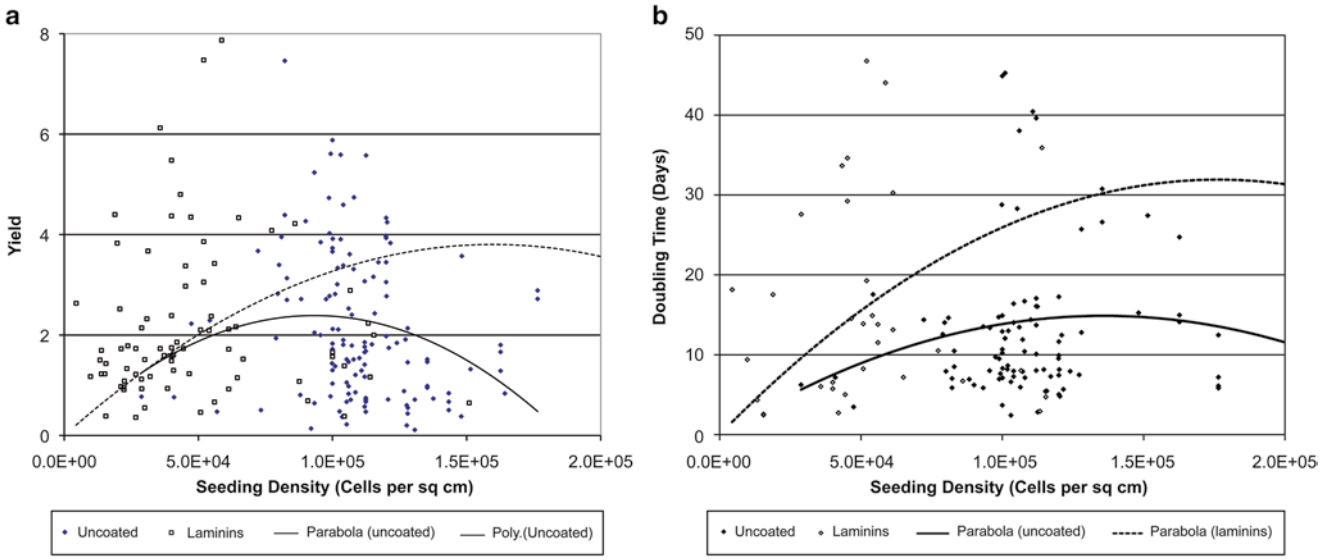

Fig. 7 Density of cells initially seeded on the growth surface. (**a**) Yield as a function of seeding density (cells/cm^2) for hNSC growth on uncoated (*filled diamond*) and laminin-coated (*square*) surfaces. The curves are fits of quadratic polynomials (parabolae) of the form yield $= a \times d^2 + b \times d$, where d is surface seeding density, to the respective data. Fits were constrained to yield = 0 at $d = 0$. Fitted parameters: uncoated surfaces (*solid line*) $a = -3.0\ (\pm 0.65) \times 10^{-10}$, $b = 5.0\ (\pm 0.47) \times 10^{-5}$; laminin-coated surfaces (*dashed line*), $a = -1.0\ (\pm 0.83) \times 10^{-10}$, $b = 5.0\ (\pm 2.33) \times 10^{-5}$. (**b**) Doubling time t_2 as a function of seeding density for hNSC growth on uncoated (*filled diamond*) and laminin-coated (*square*) surfaces. Fitted parameters for parabolae: uncoated surfaces (*solid line*) $a = -8.0\ (\pm 0.5) \times 10^{-10}$, $b = 2.0\ (\pm 0.9) \times 10^{-4}$; laminin-coated surfaces (*dashed line*) $a = -1.0\ (\pm 0.7) \times 10^{-9}$, $b = 4.0\ (\pm 3.0) \times 10^{-4}$

Table 1 Goodness-of-fit coefficients of determination R^2 for polynomials of different order fitted to yield as function of seeding density

Order	1	2	3	4	5	6
Uncoated	0.0020	0.0400	0.0853	0.1357	0.1367	0.1367
Laminin	0.0009	0.0286	0.0917	0.0983	0.1020	0.1027

$n = 6$ were fitted, R^2 did not improve beyond $n = 4$ for uncoated surfaces and $n = 5$ for laminin-coated surfaces, due to providing local maxima in the fitted curves most closely coinciding with the observed seeding density ranges producing greatest yields. The best-fitting parabola for growth on uncoated plastic was relatively sharp, extending through the data points on both upward and downward trajectories, and having its maximum at 1.2×10^5 cells/cm^2, the largest seeding density that did not result in a decrease in yield. The best-fitting parabola for laminin extended upward well beyond the actual data, peaking at 2.5×10^5 cells/cm^2, such that the observed data points were situated along the increasing portion of the curve. This suggests that plating density was less critical on laminin, consistent with the decreased tendency of cells to aggregate by enhanced interaction with the growth surface compared to uncoated surfaces. This increased surface interaction appeared to improve survival and enable growth at lower seeding densities.

Seeding surface density exerted minimal detectable effect on t_2 on both uncoated and laminin-coated plastic (Fig. 7b). Correlation coefficients between t_2 and surface density were only +0.079 on uncoated and −0.040 on laminin-coated polystyrene. This is consistent with the biphasic relationships between surface density and yield, given the inverse relation between yield and t_2 (Fig. 6). Fitting of the data to parabolae, however, while better than lines, resulted in relatively poor goodness of fit ($R^2 = 0.023$ uncoated, 0.156 laminins). Therefore, while the effect of seeding density is most pronounced on yield, it had much weaker influence on growth rate as measured by doubling time.

Discussion

Growth Patterns of fhNSC

Previous studies have established the minimal set of growth factors (basic FGF and LIF) and their concentrations necessary to sustain proliferation in chemically defined serum-free media [2, 8]. Within the context of these requirements, growth of fetal hNSC in multilayers and monolayers was studied in the present work to understand how these patterns emerge in culture and how culture parameters such as seed number and growth time determine cell yield. Each growth pattern was found to progress with a unique time course in a stereotypical series of events. These patterns were found to originate from differences between the extents to which cells

interact with each other and with the culture surface during the first few days of culture. Dynamics of fetal- and adult-derived hNSC have been quantified previously for growth in neurospheres [5] and monolayers [25]. They have also suggested extensive intercellular dynamics during growth of fhNSC in neurospheres, in which smaller aggregates of cells coalesce by "neurosphere fusion" into larger, smooth-surfaced aggregates [5]. The present study documents the extensive motile activity of fhNSC underlying dynamics of growth in multilayer and monolayer patterns to reveal how multilayers are capable of greater cellular production than either neurosphere or monolayer modes [13].

Cell Motions During Early Growth

Motions of cells both within the liquid medium and along the growth substrate were observed to be crucial for fhNSC survival, growth, and proliferation. Furthermore, elaboration of lamellipodia early in culture was found to be the most reliable indicator of cell survival and proliferation. hNSC are typically cultured on low-attachment surfaces to encourage formation of neurospheres [5], and on coated surfaces to promote monolayer formation [2, 7, 25] and to avoid serum-containing medium [11, 12]. The erratic mobility of freshly dispersed cells in the fluid phase above tissue culture-treated but otherwise uncoated plastic surfaces is reminiscent of "Brownian motion," in which the cells are randomly buffeted by water molecules and, more likely, microscopic fluctuations in convection aided by heat from the light source [22, 26]. This motion enables their coalescence into small (e.g., 20–100 cell) clusters during the first 24–72 h after plating, which is further reminiscent of neurosphere formation [5]. Instead of coalescence into larger aggregates, however, clusters were observed to attach to the culture surface resulting in the nucleation of multilayers, as though the clusters had "fused" with the surface rather than other clusters. Cells within the clusters or colonies elaborate lamellipodia within minutes of surface contact that repeatedly "sample" the substrate by rapid extension and retraction. These extension and retraction cycles occur in different directions until a fortuitous encounter with the proximate area surrounding lamellipodia extended by a neighboring cluster, which stabilizes both lamellipodia such that they are much less likely to retract. This "contact" appears to promote proliferation of cells within both clusters as well as adherence of cells to the substrate and enable exchange of cells between clusters by migration along the substrate. This early pattern explains the observations of Wakeman et al. [13] that multilayer formation is most successful by allowing freshly plated cells to remain undisturbed for 3–5 days before any movement of the culture vessel. It also explains their observed critical dependence of culture yield and proliferation rate on the surface area density of the seeded cells quantified in this study.

Substrate Attachment and Multilayer Versus Monolayer Growth

The comparative strengths of surface attachment and intercellular interactions appear to determine the subsequent pattern of growth as neurospheres, multilayers, or monolayers. Our time-lapse studies indicate that laminin coating of the surface induces a growth pattern characterized by extensive interaction with the substrate almost to the exclusion of the extensive intercellular interactions observed with neurospheres and multilayers. Freshly seeded cells were observed to attach to laminin surfaces, express lamellipodia, and begin migration along the surface within minutes of seeding. Apparent colonies form only after extensive migration and proliferation of the freely motile cells results in the diminution of free surface area, suggesting that some colonies arise as families of daughter cells lacking space to migrate away from the site of mitosis.

With weaker surface attachment, hNSC also move in the fluid phase above the substrate and readily interact with each other to create clusters. Then, depending on the strength of surface affinity, they either proliferate within the clusters to form neurospheres in the case of weakest surface attachment or simultaneously interact with both each other and the surface to create the flattened colonies that nucleate proliferation as multilayers. Cells migrate away from colonies with which they were originally associated to join either the central masses of other colonies or the cells extending along the multicellular branches that form along lamellipodia initially projected by surface-attached cells during their initial exploration of the growth substrate. Thus, the branch or chain migration originally documented by Imitola et al. [27] results from wandering cells recruited to already growing branches of their colonies of origin and other colonies.

Quantitative Parameters of Growth

Growth Time Course and the Exponential Doubling Model

One perhaps striking finding of the present study is the quantitative consistency of fetal hNSC growth dynamics in multilayers and monolayers. Earlier studies of hNSC derived from fetal telencephalon and subventricular zone between 5 and 20 weeks gestation found doubling times ranging from 7 to 21 days, dependent on cell isolate, duration of continuous culture in bFGF and LIF, and growth factor concentrations, but with averages of 12–15 days under the most optimal growth conditions [2, 25]. The present study found a similar wide range of doubling times for hNSC derived at 13 weeks, in optimally supplemented culture media, with an average of 13 days, indistinguishable from the earlier data. Therefore, these data represent proliferation dynamics characteristic of hNSC derived from this source.

Previous studies have generally used relatively constant growth periods in determination of yield, such that this effect could be masked [2, 8, 25]. By allowing growth time to vary in this study, however, it became possible to elucidate that hNSC proliferation was consistent with the simple exponential doubling model. In this model, each cell in a culture population undergoes mitosis with a constant doubling time across the entire span of culture, from seeding to increasing fluence. The results of the present study are consistent with proliferation dynamics being both uniform across the population of cells and stationary with respect to the duration of the culture. Nonetheless, given the morphological differences observed in the growth patterns of multilayers and monolayers, it is reasonable to conclude that more detailed examination of the timing of individual cell divisions, e.g., with fluorescently tagged vital nuclear markers, will be necessary to reveal the temporal fine structure of hNSC growth to test the model's assumptions.

Growth Dependence on Intercellular Interactions

Statistical analysis of growth data unsurprisingly shows that the number of harvested cells was most strongly determined by how many cells were seeded and the period of time they were allowed to grow. Absence of correlation between number of cells harvested per number seeded (yield) and the seed size, however, results from a biphasic (or higher order) relationship between yield and seed size. Since yield is ultimately determined by the proliferation rate of each cell during the culture period, this relation suggests that both positive and negative interactions between cells influence survival and proliferation.

A model incorporating competing influences is captured in an inverted parabolic relation. For example, a linear, additive model, in which each cell secretes a growth factor (at a constant rate), binding to a saturable receptor necessary for survival, produces an increased yield at greater seed number, i.e., a relation with a positive slope. If, instead, synthesis and secretion of the growth factor are dependent on the secreted growth factor, the relation becomes parabolic. As seed size increases, the cells become closer in proximity, the interaction is positive, and yield increases. Due to the saturable receptor interaction necessary for synthesis and secretion of the growth factors, however, at a critical seed size, the positive effect of increased cell density attains a maximum. Competition between the crowded cells begins to deplete the extracellular concentration of secreted growth factor, and synthesis and secretion rates become limited. Thus the effect of further crowding is a negative influence, which may include competition for nutrients and other growth modes favored by cell crowding, such as neurosphere formation that predominates at greater seed sizes [13], to decrease yield.

Wakeman et al. [13] observed that proliferation in a non-neurosphere, multilayer growth pattern in serum-free medium could be obtained by seeding fetal hNSC at a sufficiently large surface area density of ~10^5 cells/cm^2. The present work quantitatively defines the ranges of seeding densities around this optimum resulting in both maximum yields and shortest doubling times for both uncoated and laminin-coated surfaces. The optimal seeding density of 10^5 cells/cm^2 on uncoated plastic spaces each individual cell (or small aggregate) at mutual separation distances at which paracrine interactions by small diffusible growth factors are feasible. For closely packed cells (i.e., arranged on a hexagonal lattice), the average center-to center separation distance is 34 μm. For cells with an average diameter of 10 μm, the average edge-to-edge intercellular distance is thus 24 μm, which can be traversed by a 10 kDa growth factor with a diffusion constant of 1 μm^2/s in an average time of 2.5 min. As multilayers tend to form from aggregates, this intercellular separation is less important as cells within each colony are able to maintain high local concentrations of growth factors to sustain survival. With laminin coating, however, the minimum seeding density observed in this study of 10^4 cells/cm^2 places the cells with an average edge-to-edge separation distance of 98 μm, which increases the average diffusion time to 40 min. Therefore, laminin appears to relax the requirements for intercellular communication by diffusible growth factors.

Laminin

While laminins, other ECM molecules, and surface coatings are not required for culture of fetal hNSC as monolayers [1, 25], they had been regarded as necessary for growth in the absence of serum [11, 12] until discovery of the multilayer growth pattern [13]. The findings of the present study reveal that laminin-coated surfaces induce a monolayer growth pattern morphologically characterized by extensive exploration of the surface by lamellipodia almost to the exclusion of the attractive intercellular contacts that develop in multilayer and neurosphere patterns. Thus, laminin eliminates the early phase of interactions between cells necessary in multilayer culture, and intercellular interactions only appear later as proliferation decreases the available surface area. These surface interactions also appear to decrease the need for paracrine interactions between cells, as revealed by the shift in yield to greatly decreased area seeding densities and the widening of the yield curve to a much broader range of densities. Laminins and other ECM have been considered to be growth factors similar to bFGF, LIF, EGF, and others that sustain survival and proliferation, largely due to apparent sharing by integrins of signal effectors converging on mitogen-activated mitosis regulators [11, 17] sustaining NSC. The present study revealed, perhaps surprisingly, that the profound morphological effect of laminin on the fNSC growth pattern was accompanied by no increase in the proliferation rate compared to growth on uncoated plastic, as measured by the doubling time constant, or on the functional dependence of yield on the doubling time. Thus, our findings support the hypoth-

esis that laminin facilitates survival of fetal hNSC without changing cell cycle dynamics as has been observed for other artificial growth surfaces [28]. As elaboration of lamellipodia was found to be the key indicator of survival and proliferation in both monolayer and multilayer growth patterns, and laminin evokes very early expression of lamellipodia, this exploratory phenotype may promote essential metabolic processes that provide a necessary condition for proliferation on artificial substrates. It is thus noteworthy that transcriptome profiling of human neocortical germinal zones at the same period of fetal development coinciding with the isolation of hNSC used in the present study has revealed abundant expression of laminins as well as β-tubulins within areas of stem and progenitor cell self-renewal [29].

Acknowledgment This work was supported by grants from the California Institute for Regenerative Medicine.

Suggested Readings

Nethercott H, Sheridan M, Schwartz PH, Nethercott H, Sheridan M, Schwartz PH. Neural stem cell culture. In: Loring JF, Wesselschmidt RL, Schwartz PH, Loring JF, Wesselschmidt RL, Schwartz PH, editors. Human stem cell manual: a laboratory guide. San Diego, CA: Academic; 2007.

Ryder EF, Snyder EY, Cepko CL. Establishment and characterization of multipotent neural cell lines using retrovirus vector-mediated oncogene transfer. J Neurobiol. 1990;21:356–75.

Snyder EY, Deitcher DL, Walsh C, Arnold-Aldea S, Hartwieg EA, Cepko CL. Multipotent neural cell lines can engraft and participate in development of mouse cerebellum. Cell. 1992;68:33–51.

References

1. Flax JD, Aurora S, Yang C, Simonin C, Wills AM, Billinghurst LL, Jendoubi M, Sidman RL, Wolfe JH, Kim SU, Snyder EY. Engraftable human neural stem cells respond to developmental cues, replace neurons, and express foreign genes. Nat Biotechnol. 1998;16:1033–9.
2. Carpenter MK, Cui X, Hu Z-Y, Jackson J, Sherman S, Seiger A, Wahlberg LU. In vitro expansion of a multipotent population of human neural progenitor cells. Exp Neurol. 1999;158:265–79.
3. Gottlieb DI. Large-scale sources of neural stem cells. Annu Rev Neurosci. 2002;25:381–407.
4. Walsh K, Megyesi J, Hammond R. Human central nervous system tissue culture: A historical review and examination of recent advances. Neurobiol Dis. 2005;18:2–18.
5. Singec I, Quinones-Hinojosa A. Neurospheres. In: Gage FH, Kempermann G, Song H, editors. Adult neurogenesis. New York, NY: Cold Spring Harbor Press; 2008. p. 119–34.
6. Singec I, Jandial R, Crain A, Nikkah G, Snyder EY. The leading edge of stem cell therapeutics. Annu Rev Med. 2007;58:313–28.
7. Reynolds BA, Weiss S. Generation of neurons and astrocytes from isolated cells of the adult mammalian central nervous system. Science. 1992;255:1707–10.
8. Wachs F-P, Couillard-Despres S, Engelhardt M, Wilhelm D, Ploetz S, Vroeman M, Kaesbauer J, Uyanik G, Klochen J, Karl C, Tebbing J, Svendsen C, Weidner N, Kuhn HG, Winkler J, Aigner L. High efficacy of clonal growth and expansion of adult neural stem cells. Lab Invest. 2003;83:949–62.
9. Rietze RL, Reynolds BA. Neural stem cell isolation and characterization. Methods Enzymol. 2006;419:3–23.
10. Singec I, Knoth R, Meyer RP, Maciaczyk J, Volk B, Nikkhah G, Frotscher M, Snyder EY. Defining the actual sensitivity and specificity of the neurosphere assay in stem cell biology. Nat Methods. 2006;3:801–6.
11. Ray J, Raymon HK, Gage FH. Generation and culturing of precursor cells and neuroblasts from embryonic and adult central nervous system. Methods Enzymol. 1995;254:20–37.
12. Ray J. Monolayer cultures of neural stem/progenitor cells. In: Gage FH, Kempermann G, Song H, editors. Adult neurogenesis. New York, NY: Cold Spring Harbor Press; 2008. p. 135–57.
13. Wakeman DR, Hofmann MR, Redmond DE, Teng YD, Snyder EY. Long-term multilayer adherent network (MAN) expansion, maintenance, and characterization, chemical and genetic manipulation, and transplantation of human fetal forebrain neural stem cells. Curr Protoc Stem Cell Biol. 2009;Chapter 2:Unit2D.3.
14. Parker MA, Anderson JK, Corliss DA, Abraria VE, Sidman RL, Park KI, Teng YD, Cotanche DA, Snyder EY. Expression profile of an operationally-defined neural stem cell clone. Exp Neurol. 2005; 194:320–32.
15. Reynolds BA, Rietze RL. Neural stem cells and neurospheres–re-evaluating the relationship. Nat Methods. 2005;2:333–6.
16. Svendsen CN, Smith AG. New prospects for human stem-cell therapy in the nervous system. Trends Neurosci. 1999;22:357–64.
17. Rajan P, Snyder EY. Neural stem cells and their manipulation. Methods Enzymol. 2006;419:23–52.
18. Deloulme JC, Baudier J, Sensenbrenner M. Establishment of pure neuronal cultures from fetal rat spinal cord and proliferation of the neuronal precursor cells in the presence of fibroblast growth factor. J Neurosci Res. 1991;29:499–509.
19. Ray J, Gage FH. Spinal cord neuroblasts proliferate in response to basic fibroblast growth factor. J Neurosci. 1994;14:3548–64.
20. Svendsen CN, Fawcett JW, Bentlage C, Dunnett SB. Increased survival of rat EGF-generated CNS precursor cells using B27 supplemented medium. Exp Brain Res. 1995;102:407–14.
21. Wakeman DR, Hofmann MR, Teng YD, Snyder EY. Neural progenitors (Chap. 1). In: Masters JR, Palsson BØ, editors. Human adult stem cells, human cell culture, vol. 7. New York, NY: Springer Science+Business Media B.V.; 2009. p. 1–44.
22. Selmeczi D, Mosler S, Hagedorn PH, Larsen NB, Flyvbjerg H. Cell motility as persistent random motions: Theories from experiments. Biophys J. 2005;89:912–31.
23. Menezes JR, Luskin MB. Expression of neuron-specific tubulin defines a novel population in the proliferative layers of the developing telencephalon. J Neurosci. 1994;14:5399–416.
24. Liu L, Geisert EE, Frankfurter A, Spano AJ, Jiang CX, Yue J, Dragatsis I, Goldowitz D. A transgenic mouse class-III β tubulin reporter using yellow fluorescent protein. Genesis. 2007;45:560–9.
25. Vescovi AL, Snyder EY. Establishment and properties of neural stem cell clones: Plasticity in vitro and in vivo. Brain Pathol. 1999;9:569–98.
26. Pearle E, Collett B, Bart K, Bilderback D, Newman D, Samuels S. What Brown saw and you can too. Am J Phys. 2010;78:1278–89.
27. Imitola J, Raddassi K, Park KI, Mueller FJ, Nieto M, Teng YD, Frenkel D, Li D, Sidman RL, Walsh CA, Snyder EY, Khoury SJ. Directed migration of neural stem cells to sites of CNS injury by the stromal cell-derived factor 1α/CXC chemokines receptor 4 pathway. Proc Natl Acad Sci U S A. 2004;101:18117–22.

28. Nakaji-Hirabayashi T, Kato K, Iwata H. Improvement of neural stem cell survival in collagen hydrogels by incorporating laminin-derived adhesive polypeptides. Bioconjug Chem. 2012;23:212–21.
29. Fietz SA, Lachmann R, Brandl H, Kircher M, Samusik N, Schröder R, Lakshmanaperumal N, Henry I, Vogt J, Riehn A, Distler W, Nitsch R, Enard W, Pääbo S, Huttner WB. Transcriptomes of germinal zones of human and mouse fetal neocortex suggest a role of extracellular matrix in progenitor self-renewal. Proc Natl Acad Sci USA. 2012;109:11836–41.